Identification of a conserved interface of HIV-1 and FIV Vifs with Cullin 5

Qinyong Gu[1, §], Zeli Zhang[1, §], Christoph G. W. Gertzen[1, 2], Dieter Häussinger[1], Holger Gohlke[2, 3], Carsten Münk[1]

[1]Clinic for Gastroenterology, Hepatology, and Infectiology, Medical Faculty, Heinrich-Heine-University Düsseldorf, Düsseldorf, Germany. [2]Institute of Pharmaceutical and Medicinal Chemistry, Heinrich Heine University Düsseldorf, Düsseldorf, Germany. [3]John von Neumann Institute for Computing (NIC), Jülich Supercomputing Centre (JSC), and Institute for Complex Systems - Structural Biochemistry (ICS-6), Forschungszentrum Jülich GmbH, Jülich, Germany.

[§] These authors contributed equally to this work.

#Address correspondence to Carsten Münk, carsten.muenk@med.uni-duesseldorf.de

Word count abstract: 292

Word count text: 5162

Running Title: FIV Vif interaction with cullin 5

Abstract

The apolipoprotein B mRNA-editing enzyme, catalytic polypeptide-like (APOBEC3, A3) family of DNA cytidine deaminases are intrinsic restriction factors against retroviruses. In felids such as the domestic cat (*Felis catus*), the APOBEC3 (A3) genes encode for the A3Z2s, A3Z3, and A3Z2Z3 antiviral cytidine deaminases. Only A3Z3 and A3Z2Z3 inhibit viral infectivity factor (Vif)-deficient feline immunodeficiency virus (FIV). FIV Vif protein interacts with Cullin (CUL), Elongin B (ELOB), and Elongin C (ELOC) to form an E3 ubiquitination complex to induce the degradation of feline A3s. However, the functional domains in FIV Vif for interaction with Cullin are poorly understood. Here, we found that the expression of dominant-negative CUL5 prevented the degradation of feline A3s by FIV Vif, while dominant-negative CUL2 had no influence on the degradation of A3. In co-immunoprecipitation assays, FIV Vif bound to CUL5 but not CUL2. To identify the CUL5 interaction site in FIV Vif, the conserved amino acids from position 47 to 160 of FIV Vif were mutated, but these mutations did not impair the binding of Vif to CUL5. By focusing on a potential zinc-binding motif (K175– C161—C184–C187) of FIV Vif, we found a conserved hydrophobic region (174IR175) that is important for CUL5 interaction. Mutating this region also impaired the FIV Vif-induced degradation of feline A3s. Based on a structural model of the FIV Vif/CUL5 interaction, residues 52LW53 in CUL5 were identified as mediating the binding to FIV Vif. By comparing our results to the HIV-1 Vif/CUL5 interaction surface (120IR121, a hydrophobic region that is localized in the zinc-binding motif), we suggest that the CUL5 interaction surface in the diverse HIV-1 and FIV Vif is evolutionarily conserved indicating a strong structural constraint. However, the FIV Vif/CUL5 interaction is zinc-independent, which contrasts with the zinc-dependence of HIV-1 Vif.

44 **Importance**

45 Feline immunodeficiency virus (FIV), which is similar to human immunodeficiency virus (HIV)-
46 1, replicates in its natural host in T-cells and macrophages that express antiviral restriction
47 factors APOBEC3 (A3). To escape A3s, FIV and HIV induce degradation of these proteins by
48 building ubiquitination ligase complex using the viral protein Vif to connect to cellular
49 proteins, including Cullin 5. Here, we identified the protein residues that regulate this
50 interaction in FIV Vif and Cullin 5. While our structural model suggests that the diverse FIV
51 and HIV-1 Vifs use conserved residues for Cullin 5 binding, FIV Vif binds Cullin 5
52 independently of zinc in contrast to HIV-1 Vif.

53

54 **Introduction**

55 Antiretroviral APOBEC3 (A3) restriction factors are found in clade-specific numbers in
56 placental mammals (1). Interestingly, only this group of animals is a host of lentiviruses,
57 while other retroviruses are also found in animals outside placental mammals, *e.g.*, in fish,
58 reptiles, and birds. Humans encode seven A3 genes (A3A–A3D and A3F–A3H) and cats have
59 four genes (A3Z2a–A3Z2c and A3Z3) (2-4). In addition, cats express alternative splice variants
60 of A3Z2–Z3s by read-through transcription (3, 4). A3 proteins are packaged into nascent
61 lentiviral particles during virus assembly and release, if the virus does not counteract the A3
62 encapsidation. During the next round of infection, viral core-incorporated A3s deaminate
63 cytidines in the single-stranded (-) DNA generated during reverse transcription, thus causing
64 G-to-A hypermutations in the coding strand (5, 6). The best-characterized mechanism of
65 lentiviruses to prevent this strong restriction is based on a viral protein called viral infectivity
66 factor (Vif). In virus-producing cells, human immunodeficiency virus (HIV)-1 Vif targets, for
67 example, APOBEC3G (A3G) for degradation by forming an SCF (SKP1–cullin/RBX–F-box
68 protein)-like E3 ubiquitin ligase containing Cullin 5, as well as Elongin B and C (CUL5–ELOB–
69 ELOC) through a novel SOCS (suppressor of cytokine signaling) box that binds ELOC (7, 8).
70 The CUL5–SCF E3 ligase is also required for Vif activity against A3s in the related simian
71 immunodeficiency virus of macaques (SIVmac) (8). In these complexes, Vif works as a
72 substrate receptor for A3. In most cases, the interaction of Vif with A3s is species-specific,
73 and the intricate interfaces are still unresolved and a matter of ongoing investigation (9-13).

74 Feline immunodeficiency virus (FIV) also encodes a *vif* gene, and Vif is essential for the virus
75 to replicate in cats and cells that express feline A3s (3, 4, 9, 14-17). Similar to primate
76 lentiviruses, FIV Vif interacts with CUL5, ELOB, and ELOC to form an E3 complex to induce
77 degradation of feline A3s (18). However, HIV-1 and SIV Vifs also need CBF-β to stabilize and

78 form the E3 ligase complex, whereas FIV and other non-primate lentiviruses (*e.g.*, maedi-
79 visna virus (MVV), caprine arthritis encephalitis virus (CAEV), and bovine immunodeficiency
80 virus (BIV)) do not require CBF-β to induce A3 degradation (19-24). Instead, MVV Vif hijacks
81 cellular cyclophilin A (CYPA) as a cofactor to reconstitute the E3 ligase, while BIV Vif appears
82 to operate independently of any cofactors (19). Whether FIV Vif recruits any additional
83 protein to its E3 A3 complex is unclear.

84 To form an E3 ubiquitin ligase complex, HIV-1 Vif utilizes the BC box (SLQ motif) and the
85 CUL5 box (HCCH motif) to interact with Elongin B/C and Cullin 5, respectively (7, 8, 25-28).
86 CUL5 also binds to ELOC and so destabilizing the binding of ELOC to Vif by mutating the SLQ
87 motif also removes CUL5 from the E3 complex (7, 25, 27). HIV-1 Vif utilizes the HCCH motif
88 to bind zinc, which in turn is important for HIV-1 Vif-induced A3G degradation and binding to
89 CUL5 (27-32). In the HIV-1 Vif/CUL5 co-structure, the HCCH motif stabilizes Vif helix 3, which
90 contains a hydrophobic interface that is involved in the direct CUL5 interaction (33).
91 However, the interface between FIV Vif and CUL5 is unknown (18). In this study, we first
92 demonstrate that FIV Vif interacts with CUL5, not CUL2, to induce the degradation of feline
93 A3s and, secondly, identify specific residues in Vif and CUL5 that are important for this
94 binding. Our data support a conserved interaction surface of HIV-1 and FIV Vifs with CUL5.
95

96 **Materials and methods**

97 **Plasmids.** Domestic cat A3s expressing a carboxy-terminal hemagglutinin (HA) tag, were
98 described previously (3, 34). FIV-34TF10 (codon-optimized) Vif gene was inserted into
99 pcWPRE containing a C-terminal V5-tag (4, 9). All the FIV Vif mutants were produced by
100 fusion PCR and inserted into pcWPRE by using *EcoRI* and *NotI* restriction sites (11). HIV-1 Vif
101 expression plasmid with a C-terminal V5 tag was described before (4). Human A3G with a C-
102 terminal HA tag, a gift of Nathanial Landau, was previously described (35). pcDNA3-DN-
103 hCUL5-FLAG (15823) (36), pcDNA3-myc-CUL5 (19895) (37), pcDNA3-DN-hCUL2-FLAG (15819)
104 (36), pcDNA3-myc3-CUL2 (19892) (37), T7-Elongin C-pcDNA3 (19998) (38) and HA-Elongin B-
105 pcDNA3.1(+)-Zeo (20000) (39) were obtained from Addgene (Cambridge, USA). The CUL5
106 mutations were produced by fusion PCR and cloned into pcDNA3-myc-CUL5 by using *BamHI*
107 and *XbaI* to replace wildtype CUL5. The replication deficient packaging construct pFP93, a
108 gift of Eric Poeschla (40); the FIV luciferase vector pLinSin (4) and a VSV-G expression plasmid
109 pMD.G were used to produce FIV single-cycle luciferase viruses (FIV-Luc), which were
110 described previously (4).

111

112 **Cell cultures and transfections.** HEK293T cells (293T, ATCC CRL-3216) were maintained in
113 Dulbecco's high glucose modified Eagle's medium (DMEM, Biochrom, Berlin, Germany)
114 supplemented with 10% fetal bovine serum (FBS), 2 mM L-glutamine, penicillin (100 U/ml),
115 and streptomycin (100 µg/ml) at 37°C and 5% CO2. The FcaA3Z2bZ3 degradation
116 experiments were performed in 12-well plates, 2×10^5 293T cells were transfected with 300
117 ng feline A3Z2b or feline A3Z3 or A3Z2bZ3 expression plasmids together with 60 ng codon-
118 optimized FIV Vif expression plasmid, pcDNA3.1(+) was used as control, and 700 ng pcDNA3-

DN-hCUL5-FLAG or pcDNA3-DN-hCUL2-FLAG expression plasmids, pcDNA3.1(+) was used as control. To produce FIV-luciferase viruses, 293T cells were co-transfected with 300 ng FIV packaging construct, 300 ng FIV-luciferase vector, 300 ng A3 expression plasmid, 100 ng VSV-G expression plasmid, 30 ng FIV Vif expression plasmid in 12-well plates; in some experiments pcDNA3.1(+) was used instead of Vif or A3 expression plasmids. The test of interaction between CUL5 and FIV Vif, 293T cells were co-transfected with 1000 ng pcDNA3-myc-CUL5 and 1000 ng FIV Vif-V5 or FIV Vif mutants in 6-well plates; pcDNA3.1(+) was used as control. For the interaction between ELOB, ELOC and FIV Vif, 293T cells were co-transfected with 700 ng T7-Elongin C-pcDNA3, 700 ng HA-Elongin B-pcDNA3.1(+)-Zeo and 700 ng FIV Vif-V5 or FIV Vif mutants in 6-well plates; pcDNA3.1(+) was used as control. All the transfections were performed by using Lipofectamine LTX (Thermo Fisher Scientific, Schwerte, Germany) according to manufacturer's instruction. At 48 h post- transfection, cells and supernatants were collected.

For transfections in the presence of MG132 (474790, Calbiochem) and TPEN (16858-02-9, Calbiochem), the culture medium was replaced with fresh DMEM containing different concentrations of MG132 or TPEN, or dimethyl sulfoxide (DMSO). After the cells were treated for 16 h, the cell lysates were used for immunoprecipitation or immunoblotting as described below.

Antibodies. The following antibodies were used for the present study: mouse anti-hemagglutinin (anti-HA) antibody (1:7500 dilution, MMS-101P; Covance, Münster, Germany), mouse anti-V5 antibody (1:4500 dilution, MCA1360, ABDserotec, Düsseldorf, Germany), mouse anti-α-tubulin antibody (1:4000, dilution, clone B5-1-2; Sigma-Aldrich,

142 Taufkirchen, Germany), mouse anti-T7-tag monoclonal antibody (1:1000 dilution, 69522,
143 mouse monoclonal IgG2b, Merck, Germany), mouse anti-CUL-5 monoclonal antibody
144 (1:1000 dilution, sc-373822, Santa Cruz, USA), mouse anti-myc monoclonal antibody (1:100
145 dilution, MCA2200, MbD Serotec, Canada), mouse anti-flag M2 monoclonal antibody (1:1000
146 dilution, F1804, Sigma, USA). The second antibody was horseradish peroxidase-conjugated
147 rabbit anti-mouse antibody (1:10,000 α-mouse-IgG-HRP; GE Healthcare, Munich, Germany).

148

149 **Immunoprecipitation.** 293T cells were transfected with FIV Vif-V5 together with pcDNA3-
150 myc-CUL5 or T7-Elongin C-pcDNA3, HA-Elongin B-pcDNA3.1(+)-Zeo or FcaA3Z2bZ3-HA
151 expression plasmids. At 48h post-transfection, the cells were harvested and lysed in IP-lysis
152 buffer (50 mM Tris/HCl pH 8, 10% Glycerol, 0.8% NP-40, 150 mM NaCl) with protease
153 inhibitor cocktail set III (Calbiochem, Darmstadt, Germany) on ice for 20 min. Cell lysates
154 were clarified by centrifugation at 10,000g for 30 min at 4°C. The supernatant were
155 incubated with 15 µl rabbit anti-c-myc agarose affinity gel antibody beads (A7470, Sigma,
156 USA) or 15 µl rat anti-HA affinity matrix beads (16598600, Roche, USA). After 2 h incubation
157 at 4˚C in end-over-end rotation, the samples were washed 4 times with lysate buffer on ice.
158 Bound proteins were eluted by boiling the beads for 5 min at 95°C in SDS loading buffer. The
159 eluted materials were subsequently analyzed by immunoblotting. To detect the interaction
160 of FIV Vif with endogenous CUL5, 5 x 10^5 293T cells in 6-well plates were transfected with
161 wildtype FIV Vif or indicated mutant expression plasmids. The cells were harvested like
162 above, and 500 µl cell lysis were incubated with 2 µg mouse anti-V5 antibody (MCA1360,
163 ABDserotec, Düsseldorf, Germany) and 20 µl protein A/G plus agarose (Santa Cruz,
164 Heidelberg, Germany) for 4 h at 4°C in end-over-end rotation. The samples were washed 4
165 times after 4 h incubation, and bound proteins were analyzed by immunoblotting.

166

167 **Immunoblotting.** Transfected 293T cells were lysed in radioimmunoprecipitation assay
168 (RIPA) buffer (25 mM Tris-HCl [pH7.6], 150 mM NaCl, 1% NP-40, 1% sodium deoxycholate,
169 0.1% sodium dodecyl sulfate [SDS], protease inhibitor cocktail set III [Calbiochem,
170 Darmstadt, Germany]) on ice 20 min. Cell lysates were clarified by centrifugation at 10,000g
171 for 30 min at 4°C. Test proteins were boiled for 5 min at 95°C in SDS loading buffer and
172 resolved on a SDS-PAGE gel. Then, proteins were transferred onto immobilon PVDF transfer
173 membrane (IPVH 00010, Merck millipore, Germany) by semidry transfer (Bio-Rad, herclues,
174 CA) at 25 volt for 50 min. After blocking in 5% nonfat milk (A0830, PanReac AppliChem,
175 Germany), the membranes were detected with various primary antibodies against proteins
176 of interest and secondary antibodies were followed, and developed with ECL
177 chemiluminescence reagents (GE Healthcare).

178

179 **Homology Modeling.** We modeled the complex of FIV Vif and Cul5 based on the X-ray crystal
180 structure of the HIV-1 Vif and Cul5 complex as a template (33). Owing to the low sequence
181 identity between FIV and HIV-1 Vif, we performed the modeling in an iterative fashion. We
182 used ClustalW2 (33) to align the sequences, using the (T/S)LQ-BC box and the conserved
183 174IR175 motif as anchor points to guide the alignment. Next, we modeled the complex
184 employing Modeler v9.10 (41) and, subsequently, manually curated the sequence alignment
185 based on the resulting models: Accounting for a possible zinc dependency of FIV Vif,
186 cysteines in the FIV Vif sequence, which in the models were structurally close to zinc binding
187 cysteine and histidine residues in HIV-1 Vif, were aligned to these zinc binding residues in the
188 HIV-1 sequence (C113, C114, H108, and H139). Furthermore, we used information on the
189 secondary structure of FIV Vif, predicted by PSIPRED (42) to guide the manual curation of the

sequence alignment. The final model was then used to predict interacting residues. The model is accessible at the Protein Model Data Base (PMDB; https://bioinformatics.cineca.it/PMDB/main.php) with accession code: PM0081296.

Nucleotide sequence accession numbers. The FIV Vif sequences were obtained from GenBank, the accession numbers are: FIV C36 (AY600517.1); FIV 34TF10 (M25381.1); FIV PRR (M36968.1); FIV TM-2 (M59418.1); FIV Shizuoka (LC079040.1); FIV Oma (AY713445); FIV Lion B (EU117991); FIV Lion E (EU117992); FIV puma A (U03982), FIV puma B (DQ192583). The feline APOBEC3 and human APOBEC3G GenBank accession numbers are: FcaA3Z2b (AY971954), FcaA3Z3 (EU109281), FcaA3Z2bZ3 (EU109281) and HsaA3G (NM_021822).

Statistical analysis. Data are represented as the mean with SD in all bar diagrams. Statistically significant differences between two groups were analyzed using the unpaired Student's t-test with GraphPad Prism version 5 (GraphPad software, San Diego, CA, USA). A *p* value $\leq$ 0.05 was considered statistically significant: *P* value < 0.001 extremely significant (***), 0.001 to 0.01 very significant (**), 0.01 to 0.05 significant (*), > 0.05 not significant (ns).

208 **Results**

209 **CUL5 and not CUL2 is required for FIV Vif degradation of feline A3s.** A previous study
210 reported that FIV Vif interacts with Cullin 5 (CUL5) to form an E3 ubiquitin ligase complex
211 that can induce the degradation of feline A3 proteins by the proteasome (18). However, the
212 mechanism by which FIV Vif binds to CUL5 remains unclear and whether FIV Vif binds to
213 other Cullin family proteins is not known. Thus, we first investigated the interaction of FIV Vif
214 with CUL5 and CUL2. The FIV Vif used in this study was from FIV clone 34TF10, which is
215 derived from domestic cats (*Felis catus*, Fca), here referred to as FIV. To test the Vif/CUL
216 interaction, we co-immunoprecipitated (co-IP) Vif and CUL using lysates of human
217 embryonic kidney 293T cells transfected with expression plasmids for FIV Vif-V5, CUL2-myc,
218 or CUL5-myc. We detected FIV Vif in the CUL5-immunoprecipitated complex, while no FIV Vif
219 was observed in the CUL2 immunoprecipitation (Fig. 1A). CUL2 and CUL5 interact with Rbx
220 by using their C terminus that is critical for E3 ubiquitin ligase activity (See recent review
221 (43)). Dominant-negative (DN) CUL5 or DNCUL2 has a C terminal deletion, which can inhibit
222 SOCS box protein induced substrate degradation (36). Thus, we expressed the indicated
223 feline A3s together with FIV Vif and DNCUL5 or DNCUL2. Immunoblots of protein extracts
224 from transfected 293T cells were used as readout for the degradation of the respective A3
225 protein. The results showed that FIV Vif efficiently degraded all three tested feline A3s
226 (FcaA3Z2b, FcaA3Z3, and FcaA3Z2bZ3) in the absence of DNCUL5 (Fig. 1B), which is
227 consistent with previous studies (4, 11, 14). The presence of DNCUL5 enhanced the cellular
228 protein level of Vif and abolished the degradation of the A3s (Fig. 1B). In contrast, DNCUL2
229 did not affect the expression of Vif nor the Vif-dependent FcaA3Z3 and FcaA3Z2bZ3
230 degradation (Fig. 1C). However, in the presence of high level of FcaA3Z2b, expression
231 DNCUL2 slightly impaired its degradation by FIV Vif, possible due to DNCUL2-dependent

232 exhaustion of endogenous ElongB/C (Fig. 1D). Additionally, we investigated the impact of the
233 proteasome inhibitor MG132 on Vif-mediated A3 degradation. We found that the
234 degradation of FcaA3Z2bZ3 by FIV Vif was sensitive to MG132 treatment but comparably
235 less sensitive than the HIV-1 Vif-induced degradation of human A3G (Fig. 1E). The reasons
236 for these different responses to MG132 are unclear and might indicate different kinetics of
237 degradation.

238

239 **FIV Vif N-terminal residues are not essential for CUL5 binding.** A previous study suggested
240 that FIV Vif may utilize a novel mechanism for binding CUL5 (18). To investigate which
241 domain of FIV Vif is involved in the CUL5 interaction, we analyzed FIV Vif sequences from
242 different FIV strains. We found several conserved residues at the N-terminal protein region
243 (residues 53 to 132). Thus, we replaced the N-terminal conserved residues (53FI54, 57LR58,
244 61EGI63, 65WSF67, 68HTR70, 71DYY73, 74IGY76, 77VRE79, 81VAG83, 92MY93, 95YI96,
245 99PLW101, 105YRP107, 128MED130, and 132IEK134) of FIV Vif by alanines (Fig. 2A). All FIV
246 Vif mutants were co-expressed with CUL5-myc in 293T cells. FIV Vif with a TLQ-AAA mutation
247 served as a control because destroying ELOC binding destabilizes the CUL5 interaction (18).
248 Co-immunoprecipitation assays followed by immunoblots were used to evaluate the binding
249 of FIV Vif mutants to CUL5. The results showed that FIV Vif with mutations in 53FI54,
250 57LR58, and 77VRE79 bound CUL5, but the binding affinity appeared to be weaker
251 compared to the wildtype FIV Vif (Fig. 2B). These three FIV Vif mutants had similar binding
252 affinity to FcaA3Z2bZ3 (Fig. 2C) and ELOB/C (Fig. 2D). Consistent with a reduced CUL5
253 interaction, these Vif mutants partially lost the function to induce FcaA3Z2bZ3 degradation
254 (Fig. 2E). All other Vif mutants showed no change in CUL5 binding (Fig. 2B). Overall, it

255 appears that the residues in the N-terminus (53 to 132) of FIV Vif are not important for the
256 CUL5 interaction.

257

258 **Identification of determinants in the C-terminus of FIV Vif that regulate binding to CUL5.** It
259 has been shown that in HIV-1 Vif, CUL5 interacts with the C-terminal HCCH box (27, 28, 44).
260 Thus, we analyzed the C-terminal region of Vifs from different FIV strains. As in HIV-1, all FIV
261 Vifs contained a TLQ-BC box that is essential for ELOB/C binding (Fig. 3A). In addition, a KCCC
262 motif that is similar to the HCCH motif of HIV-1 Vif is found in FIV Vif. In the KCCC motif, we
263 identified a conserved hydrophobic domain (172MIIRGE177; Fig. 3A). Despite the low
264 sequence identity of only 13% in this region between FIV Vif and HIV-1 Vif, this hydrophobic
265 domain matched when the C-terminal regions of both Vifs were aligned (Fig. 3A). In the
266 complex structure of HIV-1 Vif/CUL5 (33), residues 120IR121 of HIV-1 Vif are involved in the
267 direct interaction with CUL5 (Fig. 3B). To investigate whether the equivalent hydrophobic
268 domain 172MIIRGE177 of FIV Vif is also involved in CUL5 binding , we replaced 172MI173,
269 174IR175, or 176GE177 with alanines (Fig. 3C). The binding activities of these FIV Vif mutants
270 with CUL5 were evaluated by co-IP assays. The results showed that FIV Vif 176177GE-AA
271 bound CUL5 similar to the wildtype FIV Vif and 172173MI-AA slightly impaired the FIV
272 Vif/CUL5 interaction, while 174175IR-AA impaired binding (Fig. 3C). Additionally, single point
273 mutations were introduced at 174IR175 and the I174A and R175A mutations of FIV Vif also
274 decreased the CUL5 interaction (Fig. 3C). Taken together, we conclude that the conserved
275 174IR175 motif of FIV Vif is the main CUL5 binding site.

276 Next, we tested the degradation activity of FIV Vif 174175IR-AA towards feline A3. The
277 results showed that FIV Vif 174175IR-AA did not induce degradation of co-expressed

278 FcaA3Z2bZ3 (Fig. 4A) and lost the ability to inhibit the anti-FIV activity of FcaA3Z2bZ3 (Fig.
279 4B). These data support the model that CUL5 binding of FIV Vif is essential for its antagonism
280 of feline A3s. Furthermore, we asked whether impairing the CUL5 binding sites of FIV Vif
281 affects its interaction with feline A3 and ELOB/C. To address this question, 293T cells were
282 co-transfected with expression plasmids for wildtype FIV Vif or alanine mutations of TLQ or
283 174IR175 together with expression plasmids for FcaA3Z2bZ3 or ELOB and ELOC. The
284 immunoprecipitation results indicate that alanine mutations of FIV Vif TLQ and 174IR175
285 variants did not lead to a loss of binding to FcaA3Z2bZ3 (Fig. 4C). However, the FIV Vif TLQ-
286 AAA variant lost its interaction with ELOB/C, as shown previously (18). The Vif 174175IR-AA
287 variant bound to ELOB/C similar to the wildtype FIV Vif (Fig. 4D). Together, these results
288 support that residues 174IR175 of FIV Vif are required for the interaction with CUL5.

289

290 **Modeling the FIV Vif/CUL5 complex structure.** To identify further interacting residues in the
291 FIV Vif/CUL5 complex, we built a homology model of the complex to guide mutational
292 analyses. As described in the methods section, we incorporated information of the predicted
293 secondary structure of FIV Vif and our results about the importance of residues 174IR175
294 and the TLQ-BC box for CUL5 binding when generating the sequence alignment of FIV Vif to
295 HIV-1 Vif. We did so to ameliorate the fact that the sequence identity between FIV and HIV-1
296 Vif is only 5.2%. In this way, residues corresponding to the FIV 174IR175 and TLQ-BC box
297 motifs were identified in HIV-1. The homology model of the FIV Vif/CUL5 complex showed a
298 contact of the TLQ-BC box with CUL5 and revealed a close proximity of residues 174IR175 of
299 Vif to residues 52LWDD55 of CUL5 (Fig. 5A and B). Thus, we mutated 52LW53 and 54DD55 of
300 CUL5 to alanines and tested these CUL5 variants for interaction with FIV Vif. The results
301 showed that CUL5 52LW53-AA no longer bound to FIV Vif; however, the CUL5 54DD55-AA

variant still bound Vif similar to the wildtype CUL5 (Fig. 5C). Additionally, we tested whether the CUL5 52LW53-AA mutant effects FIV Vif induced feline A3s degradation. We expressed the indicated feline A3s together with FIV Vif and the CUL552LW53-AA mutant in 293T cells. Immunoblots of protein extracts from transfected cells were used as readout for the degradation of the respective A3 protein. The results showed that FIV Vif degraded feline A3s with an unchanged efficiency in the presence of this CUL5 mutant (Fig. 5D). A model representing the FIV Vif E3 complex is shown in Fig. 5E.

The FIV Vif/CUL5 interaction is zinc-independent. Our FIV Vif/CUL5 complex model suggests that helix 3 of FIV Vif-CTD regulates the CUL5 binding (Fig. 5 and 6A). There are two positively charged lysines (K181 and K182) and several potential zinc-binding cysteines (C138, C161, C184, C187, C192, and C209) at the FIV Vif CTD (Fig. 6B). To further address the FIV Vif/CUL5 interaction properties, we mutated K181 and K182 to alanines and several potential zinc-binding residues to serine (C138S, C161S, C184S, C187S, C192S, and C209S; Fig. 6B). The immunoprecipitation results revealed that the C184S and C184C187-SS variants decreased the CUL5 interaction, but Vif mutations K181A, K182A, C187S, C138S, C161S, C192S and C209S did not affect CUL5 binding (Fig. 6C). Additionally, we tested the interaction of several FIV C-S mutants (C161S, C184S, C187S and C209S) with endogenous CUL5. The result showed that only C184S mutant lost CUL5 binding activity (Fig. 6D). We further investigated the binding property of FIV Vif C184S mutant to feline A3 and ELOB/C. The immunoprecipitation results indicate that FIV Vif C184S mutant has weaker binding affinity to FcaA3Z2bZ3 (Fig. 6E), compared with FIV Vif TLQ-AAA mutant and both, FIV Vif TLQ-AAA and C184S, lost interaction with ELOB/C (Fig. 6F). We further found that FIV Vif C161S, C184S and C187S mutants completely lost FcaA3Z2bZ3 degradation function, but the

other cysteine mutants (C138S, C192S and C209S) efficiently degraded FcaA3Z2bZ3 (Fig. 6G). Taken together, these data indicate that C184 of FIV Vif is not specific for CUL5 interaction, and we speculate that C184 may regulate the integral structure of FIV Vif.

To test the zinc dependency of the FIV Vif/CUL5 interaction, the cell-permeable zinc chelator TPEN (*N*,*N*,*N*',*N*'-tetrakis (2-pyridylmethyl) ethane-1,2-diamine) was applied in the following experiments. We first tested the effect of TPEN on FIV Vif's ability to induce the degradation of feline A3s. 293T cells were co-transfected with FIV Vif or HIV-1 Vif and FcaA3Z2bZ3 or HsaA3G and were treated with increasing amounts of TPEN. The immunoblotting results obtained from lysates of these cells indicated that FIV Vif efficiently degraded FcaA3Z2bZ3 in the presence of low concentrations of TPEN (2–4 μM), while higher concentrations of TPEN (5–8 μM) blocked the FIV Vif-induced FcaA3Z2bZ3 degradation (Fig. 7A). A similar observation was found in the HIV-1 Vif-HsaA3G degradation assay; however, 4 μM TPEN blocked the HIV-1 Vif-induced HsaA3G degradation, while this concentration of TPEN had no influence on FcaAZ2bZ3 degradation by FIV Vif (Fig. 7A and B). Because higher concentrations of TPEN may nonspecifically influence the A3 degradation, we tested the interaction of HIV-1 Vif or FIV Vif with CUL5 by co-IP assays using lysates of cells treated with 5 μM TPEN. The results showed that 5 μM TPEN repressed the HIV-1 Vif/CUL5 interaction, thus supporting the previous model that HIV-1 Vif/CUL5 interaction is regulated by zinc (Fig. 7C) (27-29, 44). In stark contrast, treatment with 5 μM TPEN did not impair the FIV Vif/CUL5 binding. These data suggest that the FIV Vif/CUL5 interaction is zinc-independent.

Discussion

348 FIV Vif interacts with CUL5, ELOB, and ELOC to form an E3 complex to induce degradation of
349 feline A3s (18). The interaction properties of FIV Vif with feline A3s and ELOB/C were
350 previously identified (9, 11, 18). However, the interface between FIV Vif and CUL5 was not
351 characterized.
352 Feline CUL5 and human CUL5 only differ in one amino acid, and this mutation does not
353 affect its interaction with FIV Vif (18). It was also shown that FIV Vif can induce the
354 degradation of feline A3s in both feline CRKF and human 293T cells, thus supporting that FIV
355 Vif can interact with human and feline CUL5 (11, 18). In this study, we first identified that
356 three FIV Vif N terminal mutants (53FI54, 57LR58, and 77VRE79) partially lost CUL5 binding,
357 compared to wildtype FIV Vif (Fig. 2B). These Vif mutants showed the capacity to induce
358 significant amounts of feline A3, however clearly less efficient than wildtype Vif. According
359 to our FIV Vif/CUL5 structural model, does the N terminus of FIV Vif not directly bind CUL5
360 (Fig. 5A). Thus, we speculate that these residues rather interact with an unknown factor that
361 regulates the FIV Vif/CUL5 binding. Indeed, a previous study suggested that FIV Vif requires
362 an unknown factor to stabilize the FIV Vif/CUL5/ELOB/C complex (19).

363 CUL5-type ubiquitin ligases have a variety of adaptors that induce degradation of different
364 cellular substrates (see recent review (43)). The adaptors of CUL5 share one common
365 domain, *i.e.*, the SOCS box, which consists of a BC box and a CUL5 box (43). The CUL5 box has
366 a common sequence, -LPθP-θ-YL, in which θ represents a hydrophobic residue, and CUL5
367 box is localized downstream of the BC box (43). Such a CUL5-like box is also found in HIV-1
368 Vif (PPLP motif), but this region does not interact with CUL5 (26, 45). In fact, HIV-1 Vif uses a
369 hydrophobic region of helix 3 to interact with CUL5 (28, 33, 44). In FIV Vif, a typical CUL5 box
370 is also missing (18). However, we found that FIV Vif, similar to HIV Vif, uses a hydrophobic
371 region of helix 3 upstream of the BC box, position 174 and 175, to interact with CUL5 (Fig. 3

372 and 5). Vif proteins are not unique in applying unusual CUL5 boxes. For example, the
373 adenovirus serotype 5 (Ad5) protein E4orf6 does not have a typical CUL5 box either, but it
374 still interacts with CUL5 and forms an E3 ligase complex to degrade p53 (46).

375 Three HIV/SIV accessory proteins (Vpr, Vpx, and Vif) bind zinc, which is essential for the
376 assembly of their E3 ligase complexes (47-49). Zinc is also required for BIV Vif/CUL2 binding,
377 while MVV Vif/CUL5 interaction does not need zinc (50). In this study, we used the cell-
378 permeable zinc chelator TPEN to investigate whether this chelator impairs the function of
379 FIV Vif or HIV-1 Vif in A3 degradation. We found that TPEN inhibited both FcaA3 and HsaA3
380 degradation induced by FIV Vif and HIV-1 Vif, respectively (Fig. 7A and B). It is important to
381 point out that high concentrations of TPEN will repress cellular pathways, such as those of
382 the cellular lysosome and autophagy (51). Thus, it is possible that high concentrations of
383 TPEN may impact upon many cellular degradation pathways. However, we found that 4 µM
384 TPEN inhibited the HIV-1 Vif-induced HsaA3G degradation, while this concentration of TPEN
385 had no influence on FcaAZ2bZ3 degradation by FIV Vif (Fig. 7A and B). In addition, the
386 presence of 5 µM TPEN did not allow the isolation of HIV-1 Vif/CUL5 complexes, whereas FIV
387 Vif/CUL5 complexes could still be detected (Fig. 7). Thus, our data support that zinc is not
388 important for the FIV Vif/CUL5 interaction, as discussed previously (18). Other studies have
389 demonstrated that TPEN treatment blocks the function of HIV-1 Vif, Vpr, and SIVmac Vpx
390 (47). These findings indicate that, in the group of lentiviruses, there are zinc-dependent (*e.g.,*
391 HIV-1, BIV) and zinc-independent (*e.g.,* FIV, MVV) Vif proteins. The inter-Vif diversity is high,
392 and HIV-1 Vif shares only around 16% and 5.2% identical residues with BIV or FIV Vif,
393 respectively. Thus, the requirement and structural consequences of zinc binding in Vifs are
394 currently unclear. However, whether other metals (Mg^{2+} or Ca^{2+}) bind FIV or MVV Vif needs
395 more investigation. The SOCS3/CUL5 and E4orf6/CUL5 interactions are also zinc-

396 independent (46, 52), which, together, indicates that zinc is not necessary for binding of
397 CUL5.

398 As the sequence of FIV Vif is 59 amino acids longer than that of HIV-1 Vif and no other
399 structural template is available, an unstructured loop is found in our model between helices
400 2 and 3 (Fig. 5A). This loop could be involved in the binding of CUL5 or other cofactors;
401 however, without a structural template, its function remains unknown. Whether this loop is
402 specific for FIV Vif requires further investigation. Despite the low sequence identity between
403 FIV and HIV-1 Vif and their difference in sequence length, our homology model of the FIV
404 Vif/CUL5 complex is apparently accurate enough to predict interacting residues between
405 these proteins. Our data from the CUL5 alanine variant of 52LW53 (Fig. 5C) and our
406 homology model suggest that the interaction between Vif and CUL5 is also mediated by a
407 hydrophobic contact. This is similar to the importance of the hydrophobic motif in the CUL5
408 BC box. In our homology model, helix 3 of Vif, which interacts with CUL5, is followed by
409 C184. This cysteine was shown to be important for CUL5 interaction, and also for feline A3 or
410 ELOB/C interaction, which differs from a previous study (18). As C184 is neither located in
411 the Vif/CUL5 interface according to our homology model nor involved in zinc binding, we
412 speculate that it might contribute to stabilizing the integral structure of FIV Vif. Overall,
413 while our model certainly cannot be expected to be a perfect structural representation of
414 the FIV Vif/CUL5 complex given the low sequence identity between FIV and HIV-1 Vif, we
415 were able to successfully predict interacting residues between the two proteins in those
416 regions with a higher sequence similarity.

417 Our data suggest that the Vif/CUL5 interaction in FIV structurally mirrors the one in HIV-1,
418 even if the zinc dependency of both interactions is different. After cross-species
419 transmissions of lentiviruses, the lentiviruses adapt to rather variable A3 proteins, which are

under positive selection. Positive selection is not seen in mammalian CUL5 and, thus, it makes sense that the mechanism by which Vif interacts with CUL5 shows evolutionarily preserved interfaces.

Acknowledgement

We thank Wioletta Hörschken for excellent technical assistance. We thank Eric Poeschla for plasmid pFP93. QG and ZZ are supported by China Scholarship Council. CM is supported by the Heinz-Ansmann foundation for AIDS research. We are grateful for computational support by the "Zentrum für Informations und Medientechnologie" at the Heinrich Heine University Düsseldorf.

Figure legends:

Figure 1. CUL5 is required for FIV Vif induced degradation of feline APOBEC3s. (A) FIV Vif interacts with CUL5, but not CUL2. myc-CUL5 or myc-CUL2 expression plasmids were co-transfected with FIV Vif-V5 expression plasmid. Cell lysates were immunoprecipitated with anti-myc beads and then analyzed by immunoblotting with anti-V5 antibody for FIV Vif and anti-myc antibody for CUL2 and CUL5. (B, C) Dominant-negative (DN)-CUL5, but not DN-CUL2, disrupts the degradation of feline A3s induced by FIV Vif. 293T cells were co-transfected with 300 ng expression plasmids for FcaA3Z2b-HA, FcaA3Z3-HA or FcaA3Z2bZ3-HA; 700 ng of DN-CUL5-FLAG or DN-CUL2-FLAG with 30 ng of FIV Vif-V5. pcDNA3.1 was used as control plasmid to replace the FIV Vif or dominant negative CUL5/2 expression plasmids. Cells were analyzed by immunoblotting using anti-HA, anti-V5, anti-CUL5, anti-Flag and anti-tubulin antibodies, respectively. (D) 293T cells were co-transfected with 50, 100 or 200 ng expression plasmids for FcaA3Z2b-HA, 700 ng of DN-CUL2-FLAG with 30 ng of FIV Vif-V5. The immunoblotting was performed as (B). (E) FIV Vif induces the degradation of FcaA3s in a proteasome-dependent manner. 293T cells were transfected with HsaA3G-HA or FcaZ2bZ3-HA; HIV-1 Vif-V5 or FIV Vif-V5 expression plasmids, pcDNA3.1 was used as empty plasmid control. The transfected cells were treated with the proteasome inhibitor MG132 (2.5, 5, 7.5 or 10 μM) or DMSO as control 36 h post transfection. Cells were harvested 12 h later (48 h after transfection) and then analyzed by immunoblotting with anti-HA, anti-V5 and anti-tubulin antibodies. The percentage of FcaA3 and HsaA3G were calculated relative to that in the absence of FIV Vif or HIV-1 Vif (set as 1.00).

Figure 2. Relevance of FIV Vif N-terminal residues for interaction with CUL5. (A) Schematic structure of FIV Vif. The numbers indicate the positions of amino acids mutated to alanines.

455 The relative positions of the feline A3Z2 and A3Z3 interaction sites (Z2 box, Z3 box) and the
456 Elongin B/C interaction site (BC box) are represented. (B) Co-immunoprecipitation of FIV Vif
457 wildtype and mutants with CUL5. myc-CUL5 or pcDNA3.1 empty plasmid were co-
458 transfected with expression plasmids for FIV Vif-V5 wildtype or FIV Vif mutants.
459 Immunoprecipitated complexes (IP) were analyzed by immunoblotting with anti-V5 for FIV
460 Vif and anti-myc for CUL5. (C, D) 293T cells were transfected with expression plasmids for
461 FcaZ2bZ3-HA, FIV Vif-V5 wildtype, indicated FIV Vif mutants or pcDNA3.1 empty plasmid (C);
462 or FIV Vif-V5 wildtype, indicated FIV Vif mutants, T7-ELOC or HA-ELOB and pcDNA3.1 empty
463 plasmid (D). Cells were harvested at 48 h after transfection, protein of cell lysates (input) and
464 immunoprecipitated complexes (IP) were analyzed by immunoblots stained with anti-V5
465 antibody for FIV Vif, anti-HA antibody for FcaZ2bZ3-HA and HA-ElonginB and anti-T7
466 antibody for T7-ElonginC. (E) 293T Cells were transfected with FcaA3Z2bZ3-HA and FIV Vif-
467 V5 wildtype or indicated FIV Vif mutant expression plasmids or pcDNA3.1 empty plasmid.
468 Cells were harvested and analyzed by immunoblotting with anti-HA, anti-V5 and anti-tubulin
469 antibodies, respectively.

470

471 **Figure 3. Identification of determinants in the C-terminus of FIV Vif that regulate binding**
472 **to CUL5.** (A) Top: Sequence alignment of FIV Vifs from different FIV strains including 34TF10,
473 C36, TM2, PRR, Shizuoka, Oma (Pallas's cats), and lion subtype E. Bottom: Sequence
474 alignment of C-terminal residues of FIV Vif (clone 34TF10) and HIV-1 Vif (clone NL4-3). KCCC:
475 a motif of FIV Vif similar to the HIV-1 Vif Zinc interaction region HCCH. Boxed region: a
476 conserved hydrophobic motif. Non-similar: black with no background; Conservative: blue
477 with cyan background; Block of similar: black with green background; identical: Ren with
478 yellow background; weakly similar: green with no background. (B) The structure of the HIV-1

479 Vif-CUL5 complex (Vif, orange; CUL5, green) (PDB entry 4N9F). A close-up view of the HIV-1
480 Vif-CUL5 interface is shown. The residues that are involved in the HIV-1 Vif-CUL5 interaction
481 are indicated. Red dashed lines represent hydrogen bonds. (C) FIV Vif residues 174IR175 are
482 important for FIV Vif interaction with CUL5. myc-CUL5 or pcDNA3.1 empty plasmids were co-
483 transfected with FIV Vif-V5 wildtype or indicated FIV Vif mutant expression plasmids.
484 Immunoprecipitated complexes (IP) were analyzed by immunoblotting with anti-V5 for FIV
485 Vif and anti-myc for CUL5.

486

487 **Figure 4. Mutating residues 174IR175 in FIV Vif does not impair interaction with FcaA3s,**
488 **ELOB and ELOC.** (A) FIV Vif 174175IR-AA mutant lost degradation activity against
489 FcaA3Z2bZ3. Cells were transfected with FcaA3Z2bZ3-HA and FIV Vif-V5 wildtype or
490 indicated FIV Vif mutant expression plasmids or pcDNA3.1 empty plasmid. Cells were
491 harvested and analyzed by immunoblotting with anti-HA, anti-V5 and anti-tubulin
492 antibodies, respectively. (B) FIV Vif 174175IR-AA mutant does not antagonize FcaA3Z2bZ3
493 antiviral activity. Single round FIVΔ*vif* luciferase reporter virions were produced in the
494 presence of feline A3 expression plasmids (FcaA3Z2bZ3) with FIV Vif wildtype or Vif mutants,
495 pcDNA3.1(+) was added as a control for feline A3 (control) and FIV Vif (vector). Infectivity of
496 reporter vectors was determined by quantification of luciferase activity in 293T cells
497 transduced with normalized amounts of viral vector particles. (C, D) FIV Vif 174175IR-AA
498 mutant still keep binding capability to FcaA3s, ELOB and ELOC. 293T cells were transfected
499 with expression plasmids for FcaZ2bZ3-HA, FIV Vif-V5 wildtype, indicated FIV Vif mutants or
500 pcDNA3.1 empty plasmid (C); or FIV Vif-V5 wildtype, indicated FIV Vif mutants, T7-ELOC or
501 HA-ELOB and pcDNA3.1 empty plasmid (D). Cells were harvested at 48 h after transfection,
502 protein of cell lysates (input) and immunoprecipitated complexes (IP) were analyzed by

503 western blots stained with anti-V5 antibody for FIV Vif, anti-HA antibody for FcaZ2bZ3-HA
504 and HA-ElonginB and anti-T7 antibody for T7-ElonginC.

505

506 **Figure 5. FIV Vif-CUL5 3D structure model.** (A) Homology model of the FIV Vif (orange)-CUL5
507 (green) complex in cartoon representation. Helices α3 and α4 of Vif are interacting with
508 CUL5. The model contains two unstructured loops (navy) before and after helix α2, as no
509 structural template is available for these regions. These loops might be important for binding
510 other parts of the complex. Residues that were subjected to mutational analysis are shown
511 in spheres representation. The region of the close up shown in B is indicated by a light plum
512 rectangle. (B) Close-up view of the homology model of the FIV Vif (orange)-CUL5 (green)
513 complex in cartoon representation, with interacting residues shown in sticks representation.
514 (C) The myc-CUL5 wildtype or indicated mutants expression plasmids were co-transfected
515 with FIV Vif-V5 wildtype expression plasmid into 293T cells. Cell lysates were
516 immunoprecipitated with anti-myc beads and then analyzed by immunoblotting with anti-V5
517 antibody for FIV Vif and anti-myc antibody for CUL5. (D) 293T cells were co-transfected with
518 expression plasmids for FcaA3Z2b-HA, FcaA3Z3-HA or FcaA3Z2bZ3-HA; CUL5-52LW53-AA
519 mutant with FIV Vif-V5. pcDNA3.1 was used as control plasmid to replace the FIV Vif or CUL5
520 expression plasmids. Cells were analyzed by immunoblotting using anti-HA, anti-V5, anti-
521 CUL5, anti-Flag and anti-tubulin antibodies, respectively. (E) Model of FIV Vif with E3 ligase
522 complex. The CUL5 interaction sites of FIV Vif (174IR175) are shown as red star.

523

524 **Figure 6. C184 of FIV Vif is essential for Vif-CUL5, Vif-FcaA3 and Vif-ELOB/C interaction** (A)
525 Close-up view of the homology model of the FIV Vif (orange)-CUL5 (green) complex in

526 cartoon representation, with residues that underwent mutational analysis shown in sticks
527 representation. These residues are: K181, K182, C184, C187 and C192 in the loop following
528 helix 3 of FIV Vif; C138 that forming a disulfide bond with C192 is also shown. (B) Sequence
529 representation of FIV Vif C terminal domain (CTD). (C) myc-CUL5 or pcDNA3.1 empty plasmid
530 was co-transfected with expression plasmids for FIV Vif-V5 wildtype or indicated FIV Vif
531 mutants. Immunoprecipitated complexes (IP) were analyzed by immunoblotting with anti-V5
532 for FIV Vif and anti-myc for CUL5. (D) 293T cells were transfected with expression plasmids
533 for FIV Vif-V5 wildtype or indicated FIV Vif mutants. Immunoprecipitated complexes (IP)
534 were analyzed by immunoblotting with anti-V5 for FIV Vif and anti-CUL5 for CUL5. (E, F) FIV
535 Vif C184S mutant lost binding capability to FcaA3s, ELOB and ELOC. 293T cells were
536 transfected with expression plasmids for FcaZ2bZ3-HA, FIV Vif-V5 wildtype, indicated FIV Vif
537 mutants or pcDNA3.1 empty plasmid (E); or FIV Vif-V5 wildtype, indicated FIV Vif mutants,
538 T7-ELOC or HA-ELOB and pcDNA3.1 empty plasmid (F). Cells were harvested at 48 h after
539 transfection, protein of cell lysates (input) and immunoprecipitated complexes (IP) were
540 analyzed by western blots stained with anti-V5 antibody for FIV Vif, anti-HA antibody for
541 FcaZ2bZ3-HA and HA-ElonginB and anti-T7 antibody for T7-ElonginC. (G) 293T cells were
542 transfected with FcaA3Z2bZ3-HA and FIV Vif-V5 wildtype or indicated FIV Vif mutant
543 expression plasmids or pcDNA3.1 empty plasmid. Cells were harvested and analyzed by
544 immunoblotting with anti-HA, anti-V5 and anti-tubulin antibodies, respectively.

545

546 **Figure 7. FIV Vif binding to CUL5 is zinc independent.** (A, B) 293T cells were transfected with
547 expression plasmids for FcaZ2bZ3-HA (A) or HsaA3G-HA (B); HIV-1 Vif-V5 or FIV Vif-V5,
548 pcDNA3.1 was used as empty plasmid control. The transfected cells were treated with zinc
549 chelator TPEN (2, 3, 4, 5, 6, 7 or 8 μM) or DMSO as control 36 h post transfection. Cells were

harvested 12 h later (48 h after transfection) and then analyzed by immunoblotting with anti-HA, anti-V5 and anti-tubulin antibodies. (C) myc-CUL5 expression plasmid was co-transfected with FIV Vif-V5 or HIV-1 Vif-V5 expression plasmids into 293T cells. The transfected cells were treated with 5 μM TPEN or DMSO 36 h post transfection. Cell lysates were immunoprecipitated with anti-myc beads and then analyzed by immunoblotting with anti-V5 antibody for FIV Vif and HIV-1 Vif, anti-myc antibody for CUL5.

References

1. **Münk C, Willemsen A, Bravo IG.** 2012. An ancient history of gene duplications, fusions and losses in the evolution of APOBEC3 mutators in mammals. BMC evolutionary biology **12:**71.
2. **LaRue RS, Andresdottir V, Blanchard Y, Conticello SG, Derse D, Emerman M, Greene WC, Jonsson SR, Landau NR, Löchelt M, Malik HS, Malim MH, Münk C, O'Brien SJ, Pathak VK, Strebel K, Wain-Hobson S, Yu XF, Yuhki N, Harris RS.** 2009. Guidelines for naming nonprimate APOBEC3 genes and proteins. Journal of virology **83:**494-497.
3. **Münk C, Beck T, Zielonka J, Hotz-Wagenblatt A, Chareza S, Battenberg M, Thielebein J, Cichutek K, Bravo IG, O'Brien SJ, Löchelt M, Yuhki N.** 2008. Functions, structure, and read-through alternative splicing of feline APOBEC3 genes. Genome biology **9:**R48.
4. **Zielonka J, Marino D, Hofmann H, Yuhki N, Löchelt M, Münk C.** 2010. Vif of feline immunodeficiency virus from domestic cats protects against APOBEC3 restriction factors from many felids. Journal of virology **84:**7312-7324.
5. **Zhang H, Yang B, Pomerantz RJ, Zhang C, Arunachalam SC, Gao L.** 2003. The cytidine deaminase CEM15 induces hypermutation in newly synthesized HIV-1 DNA. Nature **424:**94-98.
6. **Mangeat B, Turelli P, Caron G, Friedli M, Perrin L, Trono D.** 2003. Broad antiretroviral defence by human APOBEC3G through lethal editing of nascent reverse transcripts. Nature **424:**99-103.
7. **Mehle A, Goncalves J, Santa-Marta M, McPike M, Gabuzda D.** 2004. Phosphorylation of a novel SOCS-box regulates assembly of the HIV-1 Vif-Cul5 complex that promotes APOBEC3G degradation. Genes & development **18:**2861-2866.
8. **Yu X, Yu Y, Liu B, Luo K, Kong W, Mao P, Yu XF.** 2003. Induction of APOBEC3G ubiquitination and degradation by an HIV-1 Vif-Cul5-SCF complex. Science **302:**1056-1060.
9. **Zhang Z, Gu Q, Jaguva Vasudevan AA, Hain A, Kloke BP, Hasheminasab S, Mulnaes D, Sato K, Cichutek K, Häussinger D, Bravo IG, Smits SH, Gohlke H, Münk C.** 2016. Determinants of FIV and HIV Vif sensitivity of feline APOBEC3 restriction factors. Retrovirology **13:**46.
10. **Zhang Z, Gu Q, Jaguva Vasudevan AA, Jeyaraj M, Schmidt S, Zielonka J, Perkovic M, Heckel JO, Cichutek K, Häussinger D, Smits SH, Münk C.** 2016. Vif Proteins from Diverse Human Immunodeficiency Virus/Simian Immunodeficiency Virus Lineages Have Distinct Binding Sites in A3C. Journal of virology **90:**10193-10208.
11. **Gu Q, Zhang Z, Cano Ortiz L, Franco AC, Häussinger D, Münk C.** 2016. Feline Immunodeficiency Virus Vif N-Terminal Residues Selectively Counteract Feline APOBEC3s. Journal of virology **90:**10545-10557.
12. **Harris RS, Anderson BD.** 2016. Evolutionary Paradigms from Ancient and Ongoing Conflicts between the Lentiviral Vif Protein and Mammalian APOBEC3 Enzymes. PLoS pathogens **12:**e1005958.
13. **Simon V, Bloch N, Landau NR.** 2015. Intrinsic host restrictions to HIV-1 and mechanisms of viral escape. Nature immunology **16:**546-553.
14. **Stern MA, Hu C, Saenz DT, Fadel HJ, Sims O, Peretz M, Poeschla EM.** 2010. Productive replication of Vif-chimeric HIV-1 in feline cells. Journal of virology **84:**7378-7395.
15. **Shen X, Leutenegger CM, Stefano Cole K, Pedersen NC, Sparger EE.** 2007. A feline immunodeficiency virus vif-deletion mutant remains attenuated upon infection of newborn kittens. The Journal of general virology **88:**2793-2799.
16. **Yoshikawa R, Takeuchi JS, Yamada E, Nakano Y, Misawa N, Kimura Y, Ren F, Miyazawa T, Koyanagi Y, Sato K.** 2017. Feline Immunodeficiency Virus Evolutionarily Acquires Two Proteins, Vif and Protease, Capable of Antagonizing Feline APOBEC3. Journal of virology **91**.
17. **Troyer RM, Thompson J, Elder JH, VandeWoude S.** 2013. Accessory genes confer a high replication rate to virulent feline immunodeficiency virus. Journal of virology **87:**7940-7951.

18. **Wang J, Zhang W, Lv M, Zuo T, Kong W, Yu X.** 2011. Identification of a Cullin5-ElonginB-ElonginC E3 complex in degradation of feline immunodeficiency virus Vif-mediated feline APOBEC3 proteins. Journal of virology **85:**12482-12491.
19. **Kane JR, Stanley DJ, Hultquist JF, Johnson JR, Mietrach N, Binning JM, Jonsson SR, Barelier S, Newton BW, Johnson TL, Franks-Skiba KE, Li M, Brown WL, Gunnarsson HI, Adalbjornsdottir A, Fraser JS, Harris RS, Andresdottir V, Gross JD, Krogan NJ.** 2015. Lineage-Specific Viral Hijacking of Non-canonical E3 Ubiquitin Ligase Cofactors in the Evolution of Vif Anti-APOBEC3 Activity. Cell reports **11:**1236-1250.
20. **Ai Y, Zhu D, Wang C, Su C, Ma J, Ma J, Wang X.** 2014. Core-binding factor subunit beta is not required for non-primate lentiviral Vif-mediated APOBEC3 degradation. Journal of virology **88:**12112-12122.
21. **Han X, Liang W, Hua D, Zhou X, Du J, Evans SL, Gao Q, Wang H, Viqueira R, Wei W, Zhang W, Yu XF.** 2014. Evolutionarily conserved requirement for core binding factor beta in the assembly of the human immunodeficiency virus/simian immunodeficiency virus Vif-cullin 5-RING E3 ubiquitin ligase. Journal of virology **88:**3320-3328.
22. **Yoshikawa R, Takeuchi JS, Yamada E, Nakano Y, Ren F, Tanaka H, Munk C, Harris RS, Miyazawa T, Koyanagi Y, Sato K.** 2015. Vif determines the requirement for CBF-beta in APOBEC3 degradation. The Journal of general virology **96:**887-892.
23. **Jager S, Kim DY, Hultquist JF, Shindo K, LaRue RS, Kwon E, Li M, Anderson BD, Yen L, Stanley D, Mahon C, Kane J, Franks-Skiba K, Cimermancic P, Burlingame A, Sali A, Craik CS, Harris RS, Gross JD, Krogan NJ.** 2012. Vif hijacks CBF-beta to degrade APOBEC3G and promote HIV-1 infection. Nature **481:**371-375.
24. **Zhang W, Du J, Evans SL, Yu Y, Yu XF.** 2012. T-cell differentiation factor CBF-beta regulates HIV-1 Vif-mediated evasion of host restriction. Nature **481:**376-379.
25. **Yu Y, Xiao Z, Ehrlich ES, Yu X, Yu XF.** 2004. Selective assembly of HIV-1 Vif-Cul5-ElonginB-ElonginC E3 ubiquitin ligase complex through a novel SOCS box and upstream cysteines. Genes & development **18:**2867-2872.
26. **Bergeron JR, Huthoff H, Veselkov DA, Beavil RL, Simpson PJ, Matthews SJ, Malim MH, Sanderson MR.** 2010. The SOCS-box of HIV-1 Vif interacts with ElonginBC by induced-folding to recruit its Cul5-containing ubiquitin ligase complex. PLoS pathogens **6:**e1000925.
27. **Luo K, Xiao Z, Ehrlich E, Yu Y, Liu B, Zheng S, Yu XF.** 2005. Primate lentiviral virion infectivity factors are substrate receptors that assemble with cullin 5-E3 ligase through a HCCH motif to suppress APOBEC3G. Proceedings of the National Academy of Sciences of the United States of America **102:**11444-11449.
28. **Xiao Z, Xiong Y, Zhang W, Tan L, Ehrlich E, Guo D, Yu XF.** 2007. Characterization of a novel Cullin5 binding domain in HIV-1 Vif. Journal of molecular biology **373:**541-550.
29. **Mehle A, Thomas ER, Rajendran KS, Gabuzda D.** 2006. A zinc-binding region in Vif binds Cul5 and determines cullin selection. The Journal of biological chemistry **281:**17259-17265.
30. **Xiao Z, Ehrlich E, Luo K, Xiong Y, Yu XF.** 2007. Zinc chelation inhibits HIV Vif activity and liberates antiviral function of the cytidine deaminase APOBEC3G. FASEB journal : official publication of the Federation of American Societies for Experimental Biology **21:**217-222.
31. **Paul I, Cui J, Maynard EL.** 2006. Zinc binding to the HCCH motif of HIV-1 virion infectivity factor induces a conformational change that mediates protein-protein interactions. Proceedings of the National Academy of Sciences of the United States of America **103:**18475-18480.
32. **Giri K, Scott RA, Maynard EL.** 2009. Molecular structure and biochemical properties of the HCCH-Zn2+ site in HIV-1 Vif. Biochemistry **48:**7969-7978.
33. **Guo Y, Dong L, Qiu X, Wang Y, Zhang B, Liu H, Yu Y, Zang Y, Yang M, Huang Z.** 2014. Structural basis for hijacking CBF-beta and CUL5 E3 ligase complex by HIV-1 Vif. Nature **505:**229-233.

34. **Münk C, Zielonka J, Constabel H, Kloke BP, Rengstl B, Battenberg M, Bonci F, Pistello M, Löchelt M, Cichutek K.** 2007. Multiple restrictions of human immunodeficiency virus type 1 in feline cells. Journal of virology **81:**7048-7060.
35. **Mariani R, Chen D, Schröfelbauer B, Navarro F, König R, Bollman B, Münk C, Nymark-McMahon H, Landau NR.** 2003. Species-specific exclusion of APOBEC3G from HIV-1 virions by Vif. Cell **114:**21-31.
36. **Jin J, Ang XL, Shirogane T, Wade Harper J.** 2005. Identification of substrates for F-box proteins. Methods in enzymology **399:**287-309.
37. **Ohta T, Michel JJ, Schottelius AJ, Xiong Y.** 1999. ROC1, a homolog of APC11, represents a family of cullin partners with an associated ubiquitin ligase activity. Molecular cell **3:**535-541.
38. **Lonergan KM, Iliopoulos O, Ohh M, Kamura T, Conaway RC, Conaway JW, Kaelin WG, Jr.** 1998. Regulation of hypoxia-inducible mRNAs by the von Hippel-Lindau tumor suppressor protein requires binding to complexes containing elongins B/C and Cul2. Molecular and cellular biology **18:**732-741.
39. **Ohh M, Park CW, Ivan M, Hoffman MA, Kim TY, Huang LE, Pavletich N, Chau V, Kaelin WG.** 2000. Ubiquitination of hypoxia-inducible factor requires direct binding to the beta-domain of the von Hippel-Lindau protein. Nature cell biology **2:**423-427.
40. **Loewen N, Barraza R, Whitwam T, Saenz DT, Kemler I, Poeschla EM.** 2003. FIV Vectors. Methods in molecular biology **229:**251-271.
41. **Eswar N, Webb B, Marti-Renom MA, Madhusudhan MS, Eramian D, Shen MY, Pieper U, Sali A.** 2006. Comparative protein structure modeling using Modeller. Current protocols in bioinformatics **Chapter 5:**Unit-5 6.
42. **Jones DT.** 1999. Protein secondary structure prediction based on position-specific scoring matrices. Journal of molecular biology **292:**195-202.
43. **Okumura F, Joo-Okumura A, Nakatsukasa K, Kamura T.** 2016. The role of cullin 5-containing ubiquitin ligases. Cell division **11:**1.
44. **Xiao Z, Ehrlich E, Yu Y, Luo K, Wang T, Tian C, Yu XF.** 2006. Assembly of HIV-1 Vif-Cul5 E3 ubiquitin ligase through a novel zinc-binding domain-stabilized hydrophobic interface in Vif. Virology **349:**290-299.
45. **Wolfe LS, Stanley BJ, Liu C, Eliason WK, Xiong Y.** 2010. Dissection of the HIV Vif interaction with human E3 ubiquitin ligase. Journal of virology **84:**7135-7139.
46. **Luo K, Ehrlich E, Xiao Z, Zhang W, Ketner G, Yu XF.** 2007. Adenovirus E4orf6 assembles with Cullin5-ElonginB-ElonginC E3 ubiquitin ligase through an HIV/SIV Vif-like BC-box to regulate p53. FASEB journal : official publication of the Federation of American Societies for Experimental Biology **21:**1742-1750.
47. **Wang H, Guo H, Su J, Rui Y, Zheng W, Gao W, Zhang W, Li Z, Liu G, Markham RB, Wei W, Yu XF.** 2017. Inhibition of Vpx-Mediated SAMHD1 and Vpr-Mediated Host Helicase Transcription Factor Degradation by Selective Disruption of Viral CRL4 (DCAF1) E3 Ubiquitin Ligase Assembly. Journal of virology **91**.
48. **Schwefel D, Groom HC, Boucherit VC, Christodoulou E, Walker PA, Stoye JP, Bishop KN, Taylor IA.** 2014. Structural basis of lentiviral subversion of a cellular protein degradation pathway. Nature **505:**234-238.
49. **Wu Y, Zhou X, Barnes CO, DeLucia M, Cohen AE, Gronenborn AM, Ahn J, Calero G.** 2016. The DDB1-DCAF1-Vpr-UNG2 crystal structure reveals how HIV-1 Vpr steers human UNG2 toward destruction. Nature structural & molecular biology **23:**933-940.
50. **Zhang J, Wu J, Wang W, Wu H, Yu B, Wang J, Lv M, Wang X, Zhang H, Kong W, Yu X.** 2014. Role of cullin-elonginB-elonginC E3 complex in bovine immunodeficiency virus and maedi-visna virus Vif-mediated degradation of host A3Z2-Z3 proteins. Retrovirology **11:**77.
51. **Lee SJ, Koh JY.** 2010. Roles of zinc and metallothionein-3 in oxidative stress-induced lysosomal dysfunction, cell death, and autophagy in neurons and astrocytes. Molecular brain **3:**30.

52. **Kim YK, Kwak MJ, Ku B, Suh HY, Joo K, Lee J, Jung JU, Oh BH.** 2013. Structural basis of intersubunit recognition in elongin BC-cullin 5-SOCS box ubiquitin-protein ligase complexes. Acta crystallographica. Section D, Biological crystallography **69:**1587-1597.

Fig. 1

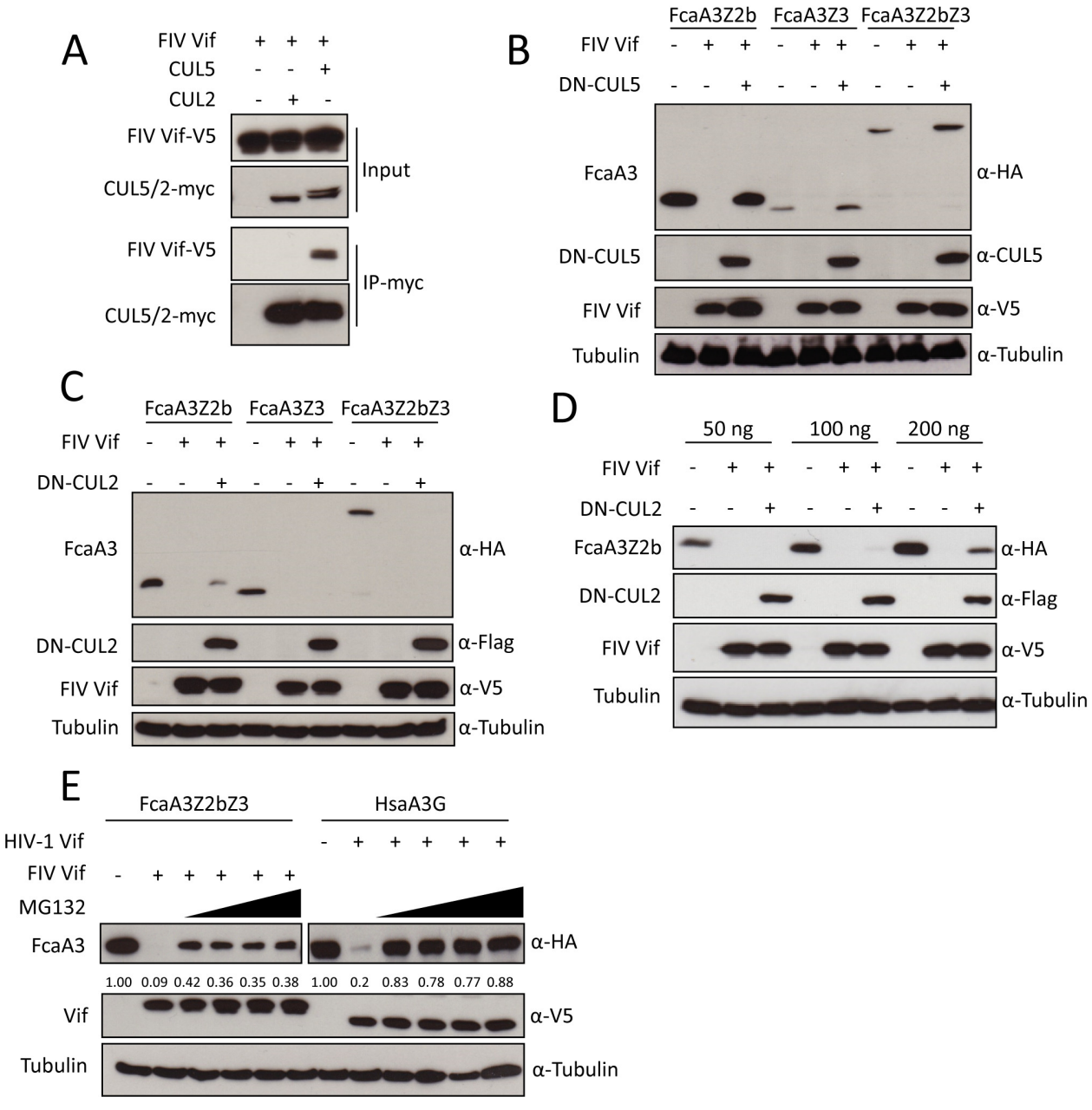

Fig. 2

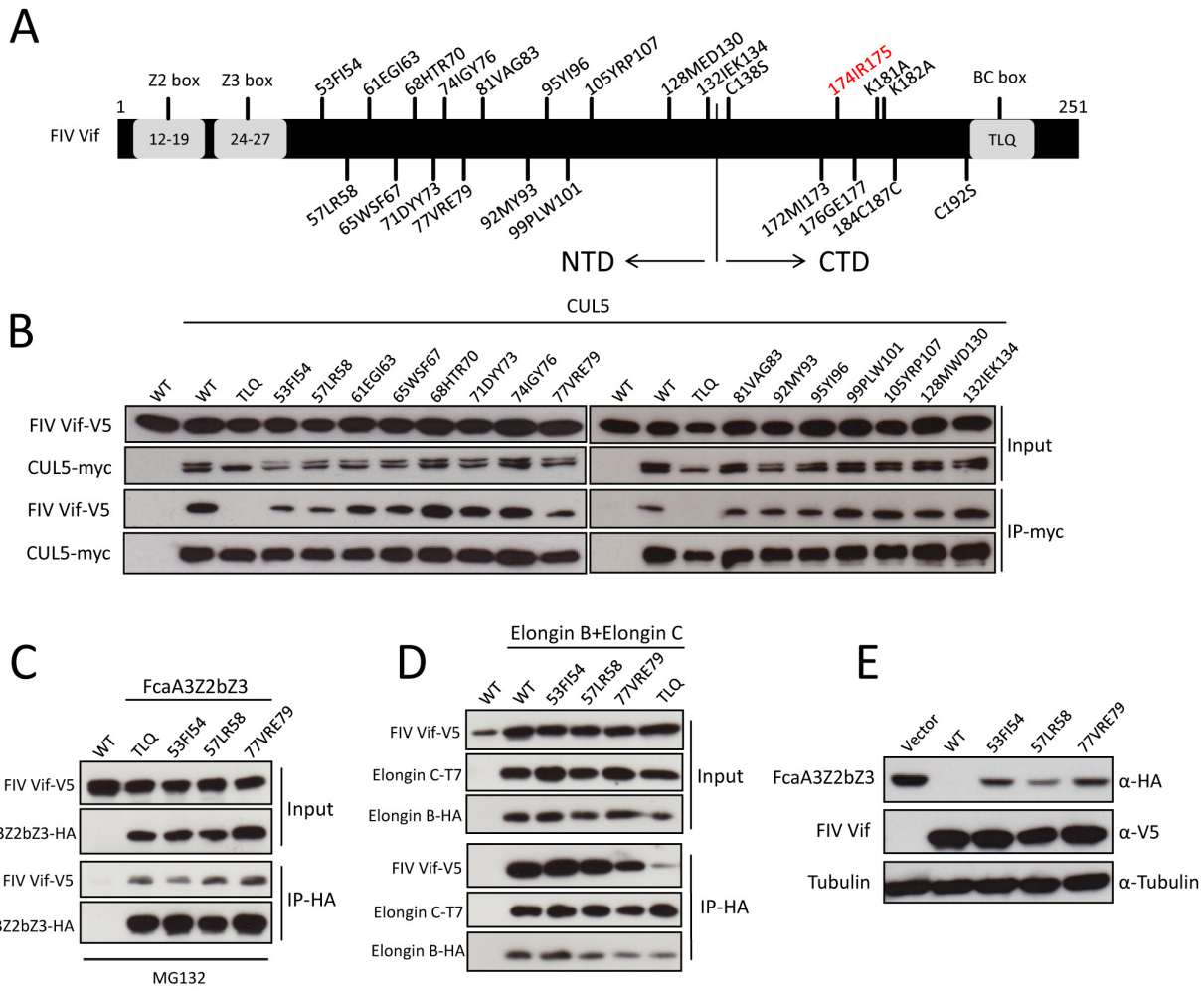

Fig. 3

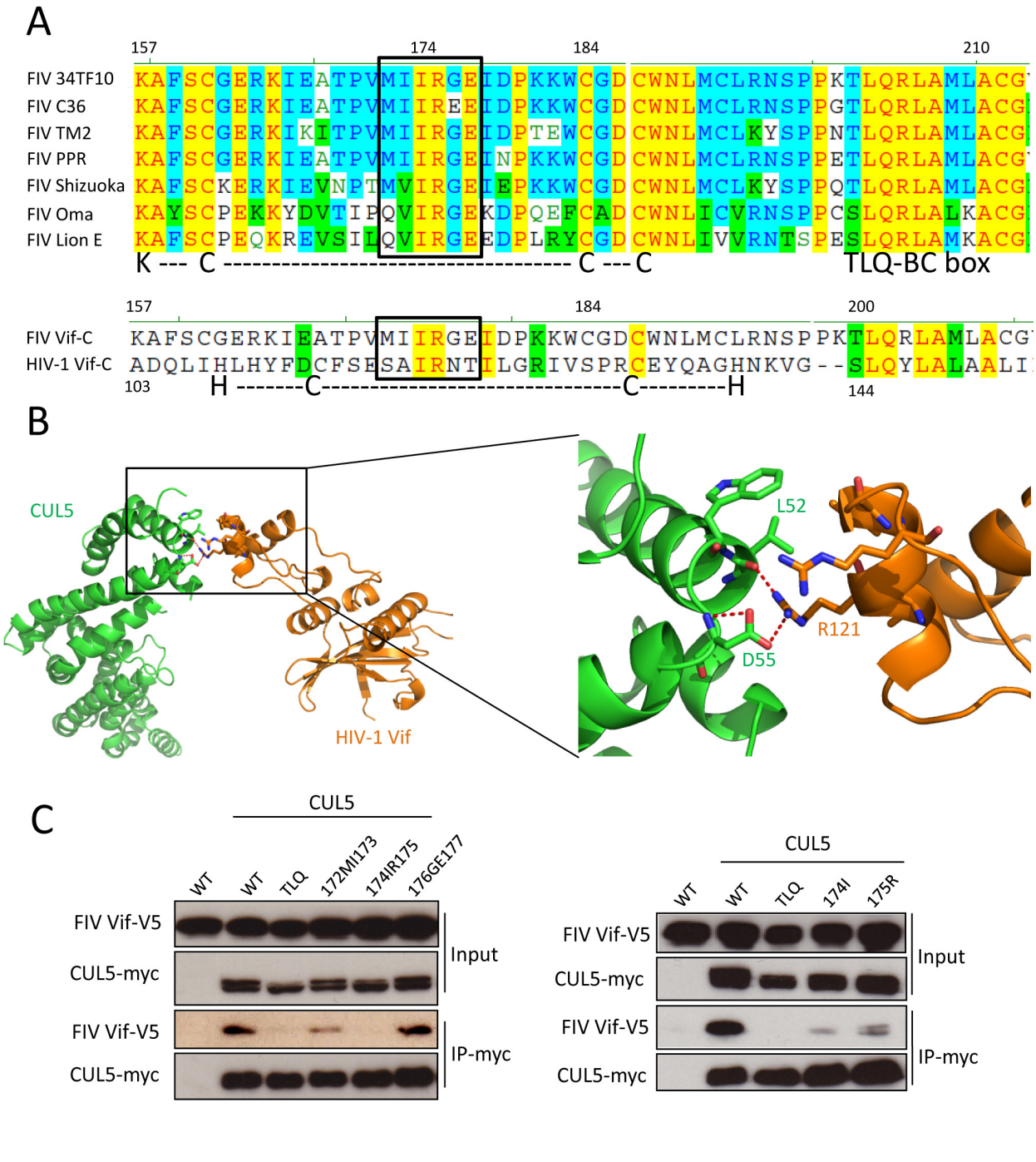

Fig. 4

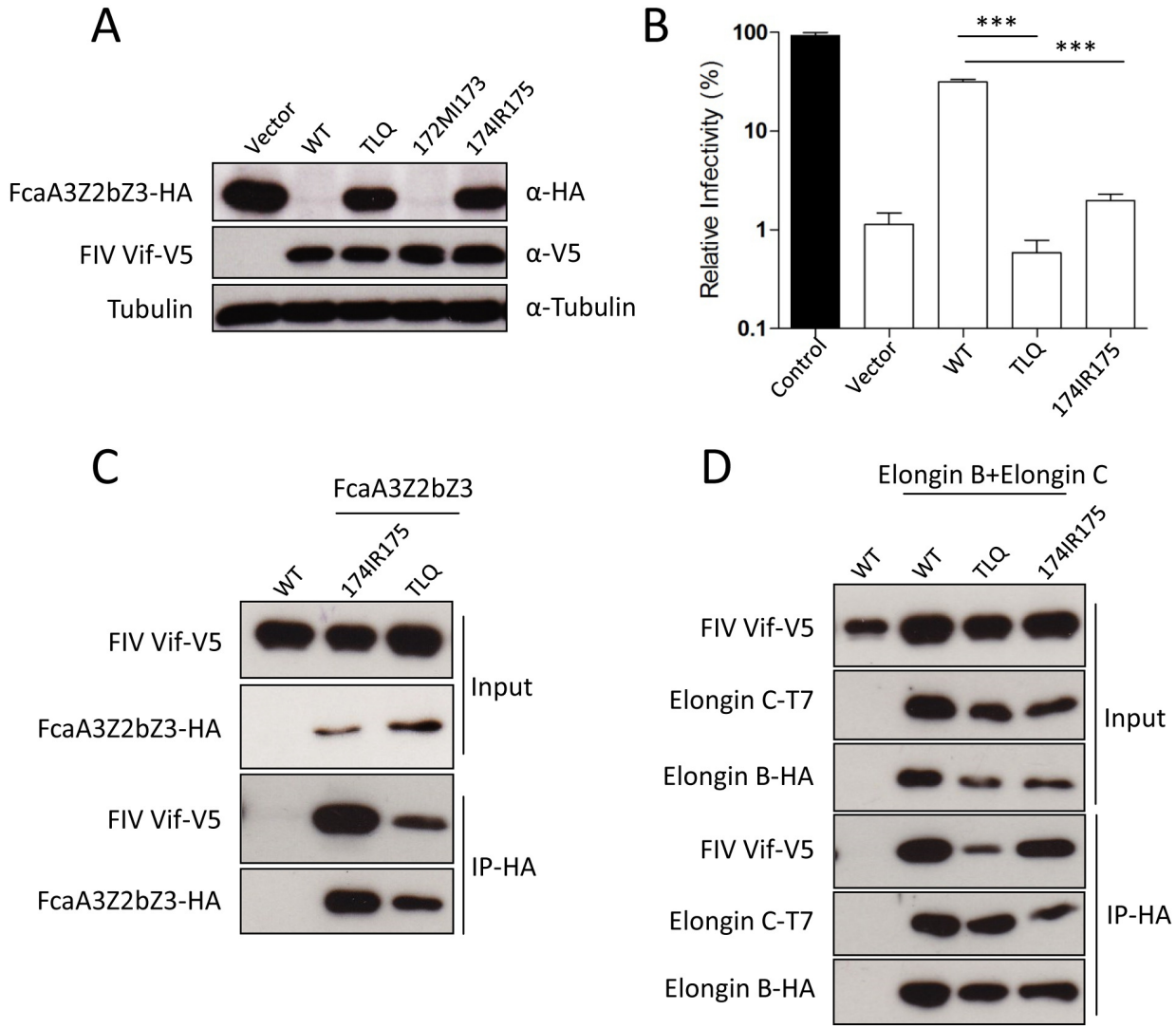

Fig. 5

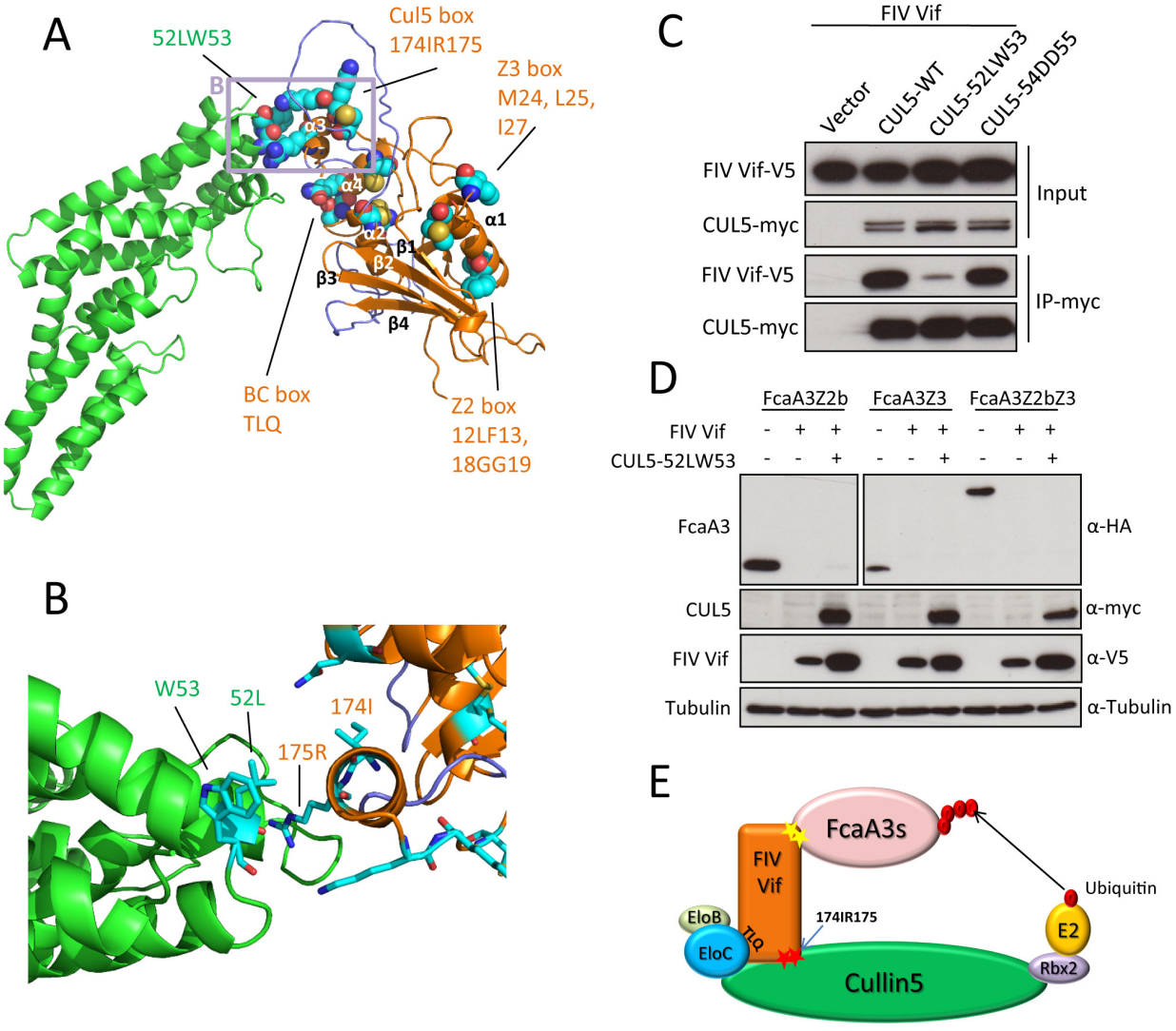

Fig. 6

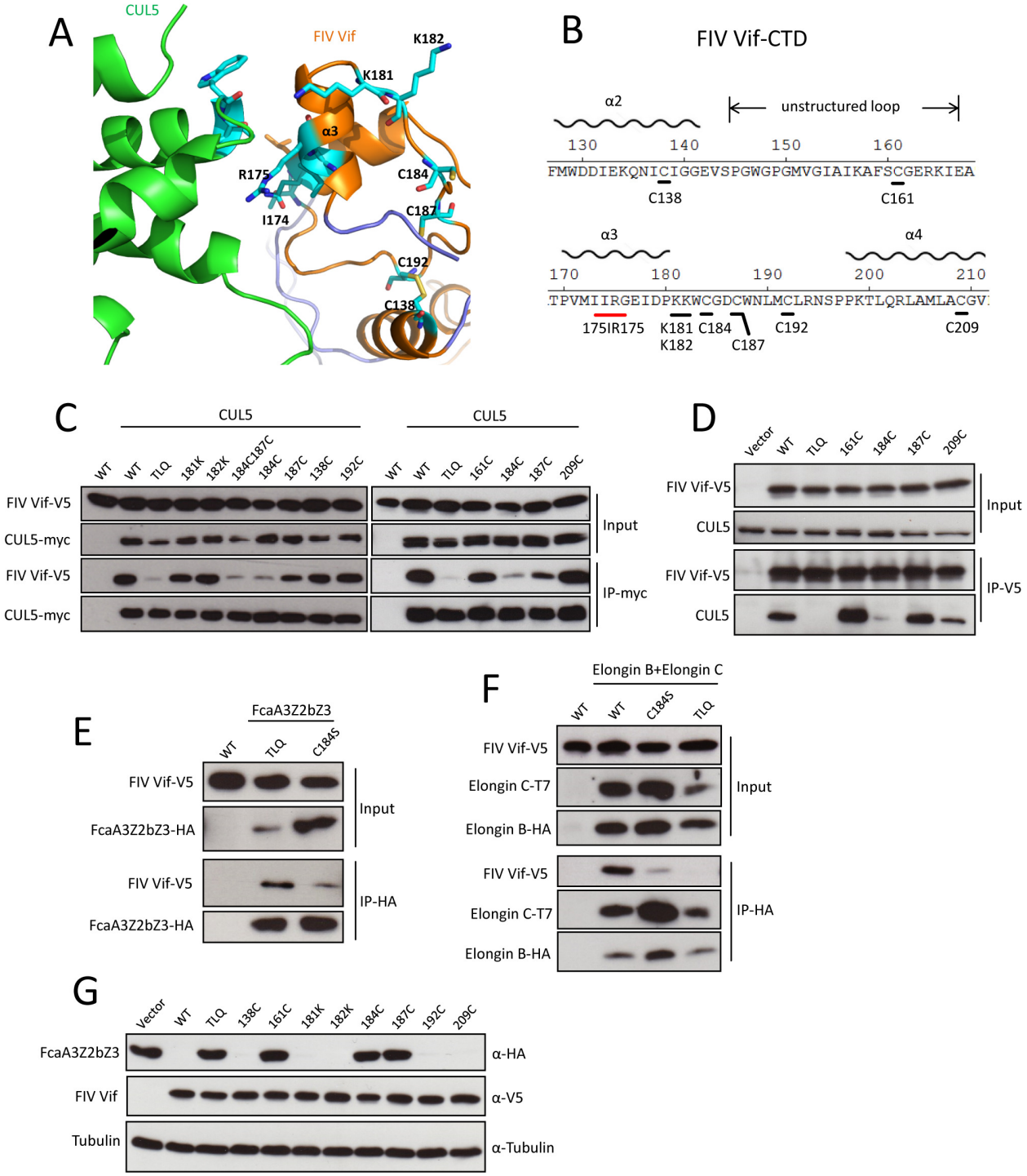

Fig. 7